



## Structure–activity relationships of heteroaromatic esters as human rhinovirus 3C protease inhibitors

Isak Im<sup>a</sup>, Eui Seung Lee<sup>b</sup>, Soo Jeong Choi<sup>a</sup>, Ju-Yeon Lee<sup>a</sup>, Yong-Chul Kim<sup>a,\*</sup>

<sup>a</sup>Research Center for Biomolecular Nanotechnology, Department of Life Science, Gwangju Institute of Science and Technology, Republic of Korea

<sup>b</sup>BK21 Center for Biomedical Human Resources, Chunnam Medical School, Chunnam National University, Republic of Korea

### ARTICLE INFO

#### Article history:

Received 26 February 2009

Revised 21 April 2009

Accepted 24 April 2009

Available online 3 May 2009

#### Keywords:

Rhinovirus

3C Protease

Heteroaromatic esters

Inhibitors

### ABSTRACT

Human rhinovirus 3C protease (HRV 3C<sup>Pro</sup>) is known to be a promising target for development of therapeutic agents against the common cold because of the importance of the protease in viral replication as well as its expression in a large number of serotypes. To explore non-peptidic inhibitors of HRV 3C<sup>Pro</sup>, a series of novel heteroaromatic esters was synthesized and evaluated for inhibitory activity against HRV 3C<sup>Pro</sup>, to determine the structure–activity relationships. The most potent inhibitor, **7**, with a 5-bromopyridinyl group, had an IC<sub>50</sub> value of 80 nM. In addition, the binding mode of a novel analog, **19**, with the 4-hydroxyquinolinone moiety, was explored by molecular docking, suggesting a new interaction in the S1 pocket.

© 2009 Elsevier Ltd. All rights reserved.

Picornaviruses include important human pathogens such as human rhinovirus (HRV), enterovirus (EV), coxsackievirus (CV), poliovirus (PV), and hepatitis A virus (HAV). HRVs are the single major cause of the common cold in populations of all ages.<sup>1,2</sup> Although rhinovirus infection is self-limiting, complications still occur in patients with asthma, congestive heart failure, bronchiectasis, and cystic fibrosis.<sup>1</sup> To date, no agent has been approved by the FDA for treatment of rhinovirus infection. In addition, the large number (>100) of known HRV serotypes makes vaccine development difficult.<sup>3</sup> Clinical treatments are directed toward relief of the most prominent symptoms of each clinical syndrome. Previous work on anti-rhinoviral therapeutic agents focused principally on capsid-binding anti-picornaviral compounds<sup>4</sup> and HRV 3C protease (3C<sup>Pro</sup>) inhibitors.<sup>5,6</sup>

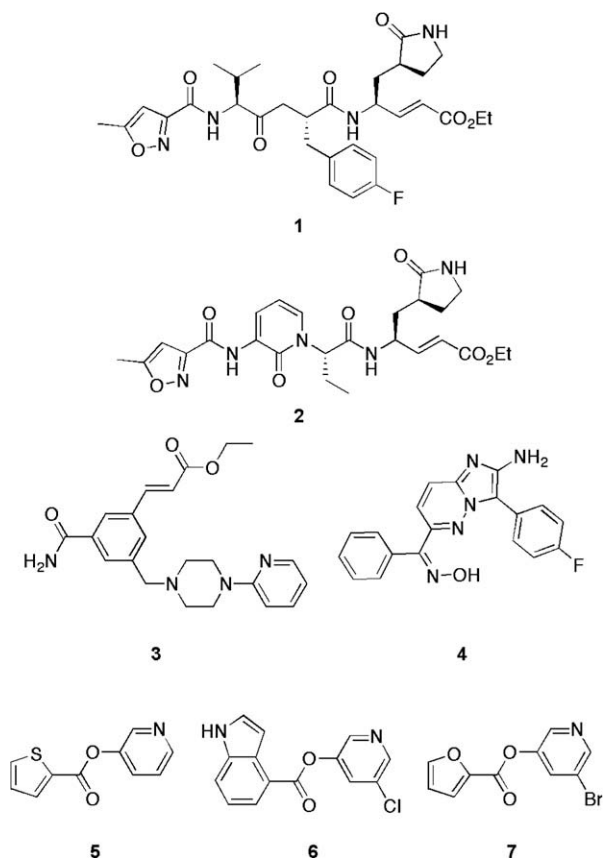
HRV 3C<sup>Pro</sup> is essential for virus replication, specifically catalyzing the cleavage of glutamine-glycine peptide bonds in a 230 kDa viral polyprotein produced by cellular translation of the viral RNA genome. HRV 3C<sup>Pro</sup> belongs to the cysteine protease family, showing structural similarity to trypsin proteases, but sharing minimal homology with common mammalian enzymes.<sup>7,8</sup> Because of the importance of the enzyme in viral replication, and the high conservation of enzyme active site components in all known HRV serotypes, potent and selective HRV 3C<sup>Pro</sup> inhibitors could be potential broad-spectrum anti-rhinoviral therapeutic agents.<sup>9–11</sup>

As part of an effort to develop HRV 3C<sup>Pro</sup> inhibitors, peptidomimetic approaches have been widely employed based on active site

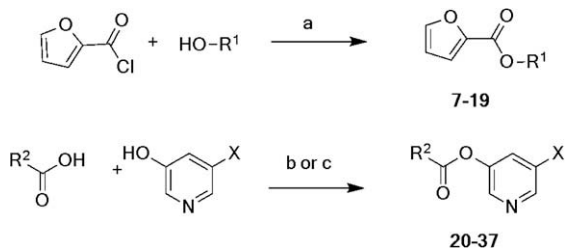
structure and cleavage specificity. To date, one peptidomimetic analog, rupintrivir (AG7088) (**1**), shown in Figure 1, is the only HRV 3C<sup>Pro</sup> inhibitor that has advanced to the stage of human clinical trials. Phase II clinical trials of rupintrivir showed that intranasal delivery reduced the mean total daily symptom score by 33%.<sup>12</sup> Recently, several efforts to develop orally bioavailable anti-rhinoviral agents have been reported; these include a rupintrivir analog, **2**,<sup>13</sup> with an improved pharmacokinetic profile, and the non-peptidic inhibitors **3** and **4**.<sup>14–16</sup>

The crystal structure of severe acute respiratory syndrome (SARS) coronavirus 3C-like protease (3CL<sup>Pro</sup>)<sup>17</sup> revealed a high similarity of active site architecture to that of HRV 3C<sup>Pro</sup>, suggesting that picornavirus 3C<sup>Pro</sup> and SARS 3CL<sup>Pro</sup> inhibitors should cross-react. In fact, SARS 3CL<sup>Pro</sup> inhibitors were developed by modifying rupintrivir<sup>18</sup> and common inhibitors with IC<sub>50</sub> values in the micromolar range were recently identified for both picornavirus 3C<sup>Pro</sup> and coronavirus 3CL<sup>Pro</sup> using high-throughput screening.<sup>19,20</sup> The pyridinyl thiophene ester **5** was discovered by screening a small molecule library (50,000 molecules) and has significant inhibitory activity against both HAV 3C<sup>Pro</sup> and SARS 3CL<sup>Pro</sup> (IC<sub>50</sub> = 0.5 μM).<sup>19,21</sup> Further work on a series of heteroaromatic esters resulted in the discovery of the most potent ester **6**, inhibiting SARS 3CL<sup>Pro</sup> with an IC<sub>50</sub> of 30 nM and an antiviral activity (EC<sub>50</sub> value) of 6.9 μM.<sup>22</sup> Another analog, **7**, also showed potent inhibition of HAV 3C<sup>Pro</sup> with an IC<sub>50</sub> of 53 nM.<sup>23</sup> Studies on the inhibitory and molecular docking mechanisms of heteroaromatic esters have shown that the 5-halopyridine moiety is crucial in binding to the S1 pocket, because both 3C<sup>Pro</sup> and 3CL<sup>Pro</sup> show high specificity for Gln as the P1 residue.<sup>23</sup>

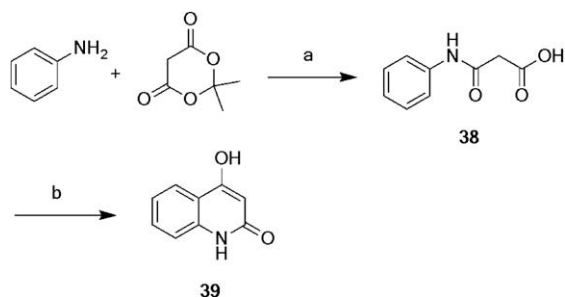
\* Corresponding author. Tel.: +82 62 970 2502; fax: +82 62 970 2484.  
E-mail address: [yongchul@gist.ac.kr](mailto:yongchul@gist.ac.kr) (Y.-C. Kim).



**Figure 1.** Structure of HRV 3C<sup>PRO</sup> inhibitors (1–4) and SARS 3CL<sup>PRO</sup> inhibitors (5–7).



**Scheme 1.** Reagents and conditions: (a) Pyridine (1.2 equiv), CH<sub>2</sub>Cl<sub>2</sub>, rt, 30 min–2 h, 30–90% yield; (b) EDC (1.2 equiv), HOBT (1.2 equiv), DIPEA (1.2 equiv), DMF, rt, 2–8 h, 50–80% yield; (c) two steps, (i) SOCl<sub>2</sub> (1.3 equiv), DMF (two drops), CH<sub>2</sub>Cl<sub>2</sub>, rt, 24 h; (ii) pyridine (1.2 equiv), CH<sub>2</sub>Cl<sub>2</sub>, rt, 30 min–2 h, 30–60% yield.



**Scheme 2.** Synthesis of 4-hydroxyquinolinone. Reagents and conditions: (a) CH<sub>2</sub>Cl<sub>2</sub>/THF, 60 °C, 9 h, 78%; (b) Eaton's reagent, 70 °C, 4 h, 72%.

Herein, we report on the structure–activity relationships of heteroaromatic esters with respect to inhibitory activity against HRV 3C<sup>PRO</sup>. Thirty-one heteroaromatic esters, including 15 newly designed derivatives, were synthesized and screened against HRV 3C<sup>PRO</sup> using a fluorescent peptide substrate. We also performed molecular docking studies to understand the potential inhibitor binding modes to the active site of HRV 3C<sup>PRO</sup>.

A general synthetic method for heteroaromatic esters is described in Scheme 1. A series of compounds was synthesized

**Table 1**  
% Inhibition and IC<sub>50</sub> values of compounds 7–19 tested against HRV16 3C<sup>PRO</sup>

7-19

Compd	R <sup>1</sup>	% Inhibition at 1 μM	IC <sub>50</sub> (μM)
7		90 ± 2	0.08 ± 0.03
8		8 ± 3	—
9		NI <sup>a</sup>	—
10		NI	—
11		87 ± 3	—
12		NI	—
13		NI	—
14		24 ± 3	—
15		NI	—
16		14 ± 6	—
17		NI	—
18		5 ± 2	—
19		98 ± 1	0.20 ± 0.05

<sup>a</sup> NI = no inhibition.

by esterification of various carboxylic acids and hydroxy-heteroaromatic groups. Initial replacement of the pyridine moiety with various heteroaromatic rings was performed with retention of the 2-furoyl group. Commercially available hydroxy-heteroaromatic rings were esterified with 2-furoyl chloride in pyridine and  $\text{CH}_2\text{Cl}_2$  (**7–18**). Compound **19** was prepared from 4-hydroxyquinolinone (**39**) in two steps (Scheme 2). The structure and inhibitory activities of furan-2-carboxylate analogs (**7–19**) are shown in Table 1. As a second series of analogs, with 5-halopyridyl esters, we used 5-chloro (or -bromo)-3-pyridinol for esterification with diverse carboxylic acid moieties. Compounds **20–29** were prepared with commercially available carboxylic acids. Compound **30** was synthesized by arylation of the -N-H group of the imidazole ring of **28**, in a reaction with 4-trifluoromethylphenyl boronic acid followed by pyridine, with use of cupric acetate and 4-Å molecular sieves in  $\text{CH}_2\text{Cl}_2$ .<sup>24</sup> The synthesis of the 2-substituted oxazole-carboxylic acids of compounds **31–35** is outlined in Scheme 3. Briefly, acylation of 2-amino diethyl malonate (**40a–e**) using various acid chlorides followed by dehydrative cyclization employing trifluoroacetic anhydride or trichloroacetyl chloride under microwave conditions at 160 °C for 5–10 min afforded the oxazoles **41a–e**,<sup>25</sup> which were subjected to basic hydrolysis to yield the corresponding oxazole-carboxylic acids **42a–e**. The structures and activities of the 5-chloro/bromopyridyl ester analogs are shown in Table 2.

A FRET-based assay system was used to measure the enzyme activity of HRV16 3C<sup>pro</sup>, expressed from cDNA<sup>26</sup>, using the fluorogenic substrate NMN-ALFQGPVK-DNP.<sup>27</sup>

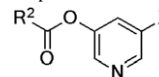
As shown in Table 1, the 5-bromopyridine moiety of compound **7**, a representative analog of the heteroaromatic inhibitors, was replaced by various heteroaromatic groups. The 3-pyridyl furonate, **8**, showed weak inhibition of HRV 3C<sup>pro</sup> (8% inhibition at 1  $\mu\text{M}$ ), whereas the 2- and 4-pyridinyl furonates, **9** and **10** showed no inhibitory effects. Chloro- and bromo-substituents at the 5 position of the pyridinyl ring significantly increased inhibitory effects (compounds **7**, **11**), with compound **7** showing the most potent activity with an  $\text{IC}_{50}$  value of 80 nM. 5-Halopyridine esters functioned well as HRV 3C<sup>pro</sup> inhibitors as a result of S1 pocket similarities with both HAV 3C<sup>pro</sup> and SARS 3CL<sup>pro</sup>.

Molecular docking of compound **7** into the active site of X-ray crystal structure of HRV 3C<sup>pro</sup> (PDB: 1CQQ) was performed by a CHARMM force field based docking tool, CDocker of Discovery Studio 2.0 (Accelrys Inc., San Diego, CA). In a rigid receptor structure, random orientations of ligand conformations were subjected to simulated annealing molecular dynamics. Final minimized poses of docked ligand were sorted by CHARMM energy (interaction energy plus ligand strain). Mass spectrometry and HPLC studies have already revealed the inhibition mechanism of heteroaromatic

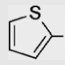
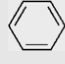
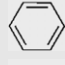
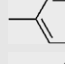
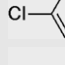
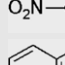
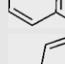
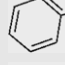
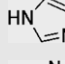
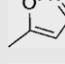
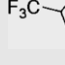

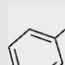

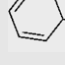
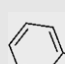
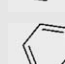
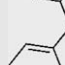
esters acting in the active site of SARS 3CL<sup>pro</sup>.<sup>20,22</sup> Such esters initially bind competitively and strongly to the active site, being

**Table 2**

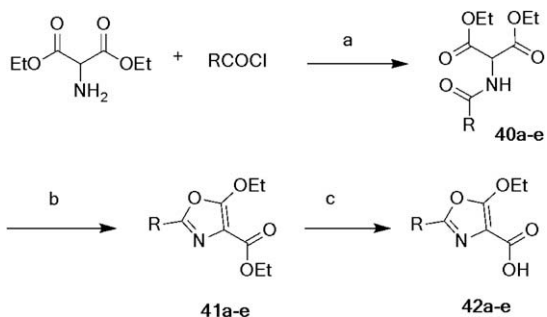
% Inhibition and  $\text{IC}_{50}$  values of compounds **20–37** tested against HRV16 3C<sup>pro</sup>



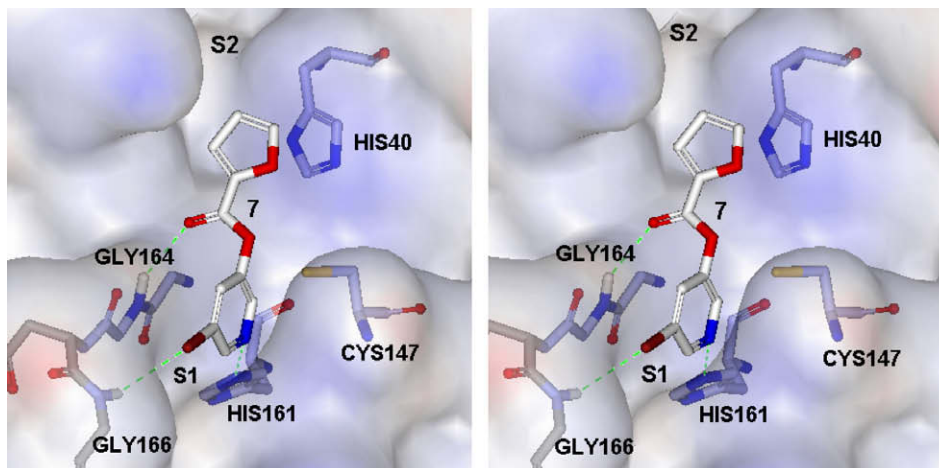
**20–37**

Compd	R <sup>2</sup>	X	% Inhibition at 1 $\mu\text{M}$	$\text{IC}_{50}$ ( $\mu\text{M}$ )
<b>20</b>		Cl	64 ± 4	—
<b>21</b>		Cl	59 ± 2	—
<b>22</b>		Cl	80 ± 4	—
<b>23</b>		Cl	79 ± 3	—
<b>24</b>		Cl	89 ± 2	—
<b>25</b>		Cl	60 ± 4	—
<b>26</b>		Cl	80 ± 10	0.71 ± 0.15
<b>27</b>		Cl	75 ± 6	—
<b>28</b>		Cl	82 ± 1	0.29 ± 0.11
<b>29</b>		Cl	NI <sup>a</sup>	—
<b>30</b>		Cl	40 ± 3	—
<b>31</b>		Cl	NI	—
<b>32</b>		Cl	5 ± 2	—
<b>33</b>		Cl	34 ± 7	—
<b>34</b>		Cl	87 ± 2	0.69 ± 0.22
<b>35</b>		Cl	5 ± 1	—
<b>36</b>		Br	34 ± 2	—
<b>37</b>		Br	63 ± 1	—

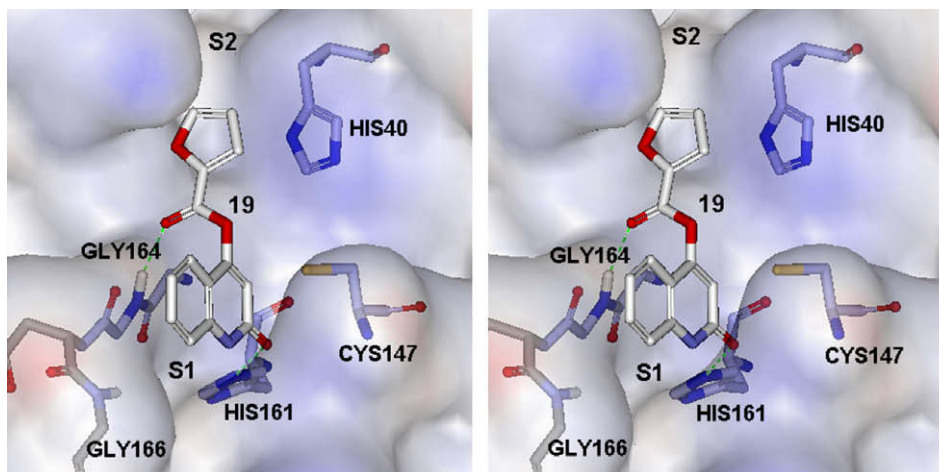
<sup>a</sup> NI = no inhibition.



**Scheme 3.** Synthesis of oxazole-4-carboxylic acids. Reagents and conditions: (a) TEA,  $\text{CH}_2\text{Cl}_2$ , R = benzoyl, phenylacetyl, 2-naphthoyl, 2,2-diphenylacetyl, or trans-cinnamoyl; 75–91%; (b) TFAA or  $\text{CF}_3\text{COCl}$ , trifluorotoluene, microwave heating, 160 °C, 5–10 min, 35–82%; (c) 10% (w/v) KOH (aq), EtOH, rt, 1 h, 65–88%.



**Figure 2.** Stereo view of initial binding mode of compound **7** with HRV 3C<sup>Pro</sup>. The nitrogen, oxygen, and sulfur atoms are colored blue, red, and orange, respectively. Hydrogen bonds are displayed as green dashed lines.



**Figure 3.** Stereo view of initial binding mode of compound **19** with HRV 3C<sup>Pro</sup>. The nitrogen, oxygen, and sulfur atoms are colored blue, red, and orange, respectively. Hydrogen bonds are displayed as green dashed lines.

recognized by S1 pocket. The carbonyl carbon is then attacked by the nucleophilic Cys residue, and become covalently connected with the protease prior to eventual release. Thus in our study, possible prehydrolysis-binding complex models of **7** was generated (Fig. 2). The lone pair electron of nitrogen moiety of 5-bromopyridine in **7** occupies the S1 binding pocket, forming a hydrogen bond with N<sup>ε2</sup> of His161 (3.1 Å). The bromo group occupies S1 pocket near the protein surface and, notably, a hydrogen bond with the –NH of Gly166 (3.0 Å) was observed, explaining the importance of the presence of a halogen group on the pyridine ring. The ester carbonyl oxygen forms a hydrogen bond with the –NH of Gly164 (2.5 Å). This predicted binding model is consistent with the binding mode of halopyridinyl esters to SARS 3CL<sup>Pro</sup> and HAV 3C<sup>Pro</sup>.

To explore the possibility of new binding interaction, new motives for the substitution of 2-position of the pyridine ring were designed for pointing toward N<sup>ε2</sup> of His161 in S1 pocket. Therefore, 2-substituted pyridinyl compounds (**12**–**16**) were investigated. Amine (**14**) and amide (**16**) substituted compounds showed moderate activity at 1 μM in the absence of chlorine at the 5 position.

The new S1 pocket binding moiety was also evaluated using *para*, *meta* benzamide (**17**, **18**) and 4-quinolinone (**19**), instead of 5-halopyridine. Compounds **17**–**19** may possibly mimic Gln, the substrate cleavage moiety. While **17** showed weak inhibitory

effect (5% inhibition at 1 μM, 21% inhibition at 10 μM), it was notable that compound **19** showed a potent inhibitory effect at 1 μM (98% inhibition), with an IC<sub>50</sub> value of 200 nM.

To gain molecular insight into the binding mode of the 4-quinolinone moiety, compound **19** was also docked in the HRV 3C<sup>Pro</sup> active site (Fig. 3). The oxygen of quinolinone forms a hydrogen bond with N<sup>ε2</sup> of His161 (2.8 Å) and the benzene ring of quinolinone occupies the outer space of the S1 pocket as does the bromo group of 5-bromopyridine, but there is no hydrogen bond with the –NH of Gly166. The hydrogen bond of the ester carbonyl oxygen with the –NH of Gly164 (2.0 Å) was also conserved as well. Although there is different spatial position of the 4-quinolinone carbonyl oxygen from the pyridyl nitrogen of **7**, the requirement of hydrogen bond angle between the carbonyl oxygen and N<sup>ε2</sup> of His161 was satisfied with the ideal hydrogen bond at 30–60° to the O=C axis within 30° of the carbonyl plane, while the sp<sup>2</sup> lone pair of pyridyl nitrogen of **7** is lying toward N<sup>ε2</sup> of His161 forming optimal hydrogen bond angle (180°). This precise hydrogen bond with His161 seems to be the key initial binding unit which mimics the Gln moiety (the P1 residue), which resulted in the dramatic inhibitory activity changes depending on the substituents R<sup>1</sup>. Interaction energy of compound **7**–**19** with 3C<sup>Pro</sup> was calculated by DOCKER program. The most potent compounds **7** and



**19** showed  $-24.5$  and  $-26.3$  kcal/mol, respectively. Comparison of the interaction energy of the *ortho* (**9**,  $-21.9$  kcal/mol), *meta* (**8**,  $-22.2$  kcal/mol), and *para* (**10**,  $-20.0$  kcal/mol) position of the pyridine nitrogen showed a parallel results with the biological activities, suggesting that the *meta* position could prefer the orientation for the hydrogen bond. Compound **12–16** with additional hydrogen bond acceptor at 2-position of the pyridine ring might disturb the optimal hydrogen bond of the pyridyl nitrogen showing the less interaction energies ( $-19.9$  kcal/mol to  $-23.5$  kcal/mol). Although weak inhibitors of benzamide analogs, **17–18** could form hydrogen bonds with His161 ( $-24.2$  kcal/mol for **17**,  $-22.6$  kcal/mol for **18**), the distance between ester carbonyl carbon and the nucleophilic  $-SH$  group of Cys might be changed unfavorably resulting in weak or no inhibitory activity.

To search for effective moieties other than the 2-furoyl group, a series of 5-halo-pyridinyl esters from various carboxylic acids was synthesized and tested. This  $R^2$  carboxylic acids were expected to provide site specificity at S2 hydrophobic pocket and affect the covalently connected binding mode at the active site. Most compounds showed moderate-to-good inhibitory effects at  $1 \mu\text{M}$  except for **29** and **31** (Table 2). Compounds with thiophen-2-carbonyl (**20**), benzoyl (**21**), phenylpropanoyl groups (**36**), and cinnamoyl (**37**) showed lower activities than did the 2-furoyl analogs (**7** and **11**). Substitution of the 5 position of the furan ring with aromatic groups allowed retention of good activity (**22–25**). The steric effect of the additional aromatic groups could stabilize the post-reaction state by  $\pi$ -stacking interaction with His40<sup>22</sup> rather than tight binding to S2 pocket. The 2-naphthoyl (**26**), 1-naphthoyl (**27**), and imidazole (**28**) groups were useful building blocks, showing potent inhibitory activities ( $IC_{50}$  of 290 nM for **28**). However, arylation of the imidazole ring of **28** showed twofold decrease in activity (**30**), which could be caused by unfavorable constraint compared to furan ring.

In further efforts to replace the furoyl ring with other heterocyclic carboxylate moieties, isoxazole and oxazole groups were investigated. In the case of 3-methylisoxazole derivative, **29**, the replaced position of furan oxygen by carbon atom resulted in the loss of activity significantly. However, oxazole derivatives (**31–35**) demonstrated a broad range of inhibitory activities depending on substitutions at the 2 position of the oxazole group. A cinnamylloxazole analog, **34**, showed the highest activity among these compounds with 87% inhibition at  $1 \mu\text{M}$  and an  $IC_{50}$  value of 690 nM. Lower electron density of oxazol ring may result in weaker binding affinity than furan or imidazol moiety, but additional hydrophobic phenyl group in a proper position connected to 2-oxazolic position with two carbon chain (**34**) significantly enhanced the inhibitory activity compared to the compounds with shorter chains or bulky aromatic groups (**31–33**, **35**).

In conclusion, 31 heteroaromatic esters were synthesized and screened as non-peptidic inhibitors against HRV 3C<sup>pro</sup>. Compound **7**, which was one of the most potent inhibitors in an earlier series, with activity against both SARS 3CL<sup>pro</sup> and HAV 3C<sup>pro</sup>, was also found to be the most potent in the current work ( $IC_{50}$  of 80 nM). Substitution of 5-halopyridine with various heteroaromatic rings resulted in the discovery of the 4-quinolinone group as an alternative key structure. Further optimization of 4-quinolinone ester analogs as Gln skeleton mimics is underway, with the aim of enhancing inhibitory activities.

## Acknowledgments

This study was supported by a grant of the National R&D Program for Cancer Control, Ministry of Health & Welfare, Republic of Korea (0720430). We thank Dr. Wai-Ming Lee (School of

Medicine and Public Health, University of Wisconsin, Madison, WI) for supplying us with cDNA encoding HRV16.

## References and notes

- (a) Couch, R. B., 3rd ed. In *Fields Virology*; Fields, B. N., Knipe, D. M., Howley, P. M., Chanock, R. M., Monath, T. P., Melnick, J. L., Roizman, B., Eds.; Lippincott-Raven: Philadelphia, 1996; Vol. 1, p 713. Chapter 23; (b) McKinlay, M. A.; Pevear, D. C.; Rossmann, M. G. *Annu. Rev. Microbiol.* **1992**, *46*, 635; (c) Phillpotts, R. J.; Tyrrell, D. A. J. *Br. Med. Bull.* **1985**, *41*, 386; (d) Gwaltney, J. M. In *Principles and Practices of Infectious Diseases*; Mandell, G. L., Douglas, R. G., Bennett, J. E., Eds.; John Wiley & Sons: New York, 1985; p 351. Chapter 38; (e) Gwaltney, J. M. In *Viral Infections of Humans*; Evans, A. S., Ed.; Plenum: New York, 1982; p 491. Chapter 20.
- (a) Rueckert, R. R., 3rd ed. In *Fields Virology*; Fields, B. N., Knipe, D. M., Howley, P. M., Chanock, R. M., Monath, T. P., Melnick, J. L., Roizman, B., Eds.; Lippincott-Raven: Philadelphia, 1996; Vol. 1, p 609. Chapter 21; (b) Kräusslich, H.-G.; Wimmer, E. *Annu. Rev. Biochem.* **1988**, *57*, 701.
- Phillpotts, R. J.; Tyrrell, D. A. *Br. Med. Bull.* **1985**, *41*, 386.
- Guiles, J. W. *Exp. Opin. Ther. Pat.* **1997**, *7*, 123.
- Wang, Q. M. *Prog. Drug. Res.* **1999**, *52*, 197.
- Wang, Q. M.; Chen, S. H. *Curr. Protein Pept. Sci.* **2007**, *8*, 19.
- Leong, L. E. C.; Walker, P. A.; Porter, A. G. *J. Biol. Chem.* **1993**, *268*, 25735.
- Matthews, D. A.; Smith, W. W.; Ferre, R. A.; Condon, B.; Budahazi, G.; Sisson, W.; Villafraña, J. E.; Janson, C. A.; McElroy, H. E.; Gribskov, C. L.; Worland, S. *Cell* **1994**, *77*, 761.
- Witherell, G. *Curr. Opin. Investig. Drugs* **2000**, *1*, 297.
- Dragovich, P. S. *Exp. Opin. Ther. Pat.* **2001**, *11*, 177.
- Leung-Toung, R.; Zhao, Y.; Li, W.; Tam, T. F.; Karimian, K.; Spino, M. *Curr. Med. Chem.* **2006**, *13*, 547.
- Hayden, F. G.; Turner, R. B.; Gwaltney, J. M.; Chi-Burris, K.; Gersten, M.; Hsyu, P.; Patick, A. K.; Smith, G. J.; Zalman, L. S. *Antimicrob. Agents. Chemother.* **2003**, *47*, 3907.
- Dragovich, P. S.; Prins, T. J.; Zhou, R.; Johnson, T. O.; Hua, Y.; Luu, H. T.; Sakata, S. K.; Brown, E. L.; Maldonado, F. C.; Tuntland, T.; Lee, C. A.; Fuhrman, S. A.; Zalman, L. S.; Patick, A. K.; Matthews, D. A.; Wu, E. Y.; Guo, M.; Borer, B. C.; Nayyar, N. K.; Moran, T.; Chen, L.; Rejto, P. A.; Rose, P. W.; Guzman, M. C.; Dovalants, E. Z.; Lee, S.; McGee, K.; Mohajeri, M.; Liese, A.; Tao, J.; Kosa, M. B.; Liu, B.; Batugo, M. R.; Gleeson, J. P. R.; Wu, Z. P.; Liu, J.; Meador, J. W.; Ferre, R. A. *J. Med. Chem.* **2003**, *46*, 4572.
- Reich, S. H.; Johnson, T.; Wallace, M. B.; Kephart, S. E.; Fuhrman, S. A.; Worland, S. T.; Matthews, D. A.; Hendrickson, T. F.; Chan, F.; Meador, J. J.; Ferre, R. A.; Brown, E. L.; DeLisle, D. M.; Patick, A. K.; Binford, S. L.; Ford, C. E. *J. Med. Chem.* **2000**, *43*, 1670.
- Hamdouchi, C.; Sanchez-Martinez, C.; Gruber, J.; Del Prado, M.; Lopez, J.; Rubio, A.; Heinz, B. A. *J. Med. Chem.* **2003**, *46*, 4333.
- Maugeri, C.; Alisi, M. A.; Apicella, C.; Cellai, L.; Dragone, P.; Fioravanzo, E.; Florio, S.; Furlotti, G.; Mangano, G.; Ombrato, R.; Luisi, R.; Pompei, R.; Rincicotti, V.; Russo, V.; Vitiello, M.; Cazzolla, N. *Bioorg. Med. Chem.* **2008**, *16*, 3091.
- Anand, K.; Ziebuhr, J.; Wadhwani, P.; Mesters, J. R.; Hilgenfeld, R. *Science* **2003**, *300*, 1763.
- Ghosh, A. K.; Xi, K.; Grum-Tokars, V.; Xu, X.; Ratia, K.; Fu, W.; Houser, K. V.; Baker, S. C.; Johnson, M. E.; Mesecar, A. D. *Bioorg. Med. Chem. Lett.* **2007**, *17*, 5876.
- Blanchard, J. E.; Elowe, N. H.; Huitema, C.; Fortin, P. D.; Cechetto, J. D.; Eltis, L. D.; Brown, E. D. *Chem. Bio.* **2004**, *11*, 1445.
- Kuo, C. J.; Liu, H. G.; Lo, Y. K.; Seong, C. M.; Lee, K. I.; Jung, Y. S.; Liang, P. H. *FEBS Lett.* **2009**, *583*, 549.
- Zhang, J.; Pettersson, H. I.; Huitema, C.; Niu, C.; Yin, J.; James, M. N. G.; Eltis, L. D.; Vederas, J. C. *J. Med. Chem.* **2007**, *50*, 1850.
- Ghosh, A. K.; Gong, G.; Grum-Tokars, V.; Mulhearn, D. C.; Baker, S. C.; Coughlin, M.; Prabhakar, B. S.; Sleeman, K.; Johnson, M. E.; Mesecar, A. D. *Bioorg. Med. Chem. Lett.* **2008**, *18*, 5684.
- Huitema, C.; Zhang, J.; Yin, J.; James, M. N. G.; Vederas, J. C.; Eltis, L. D. *Bioorg. Med. Chem.* **2008**, *16*, 5761.
- Lam, P. Y. S.; Clark, C. G.; Saubern, S.; Adams, J.; Winters, M. P.; Chan, D. M. T.; Combs, A. *Tetrahedron Lett.* **1998**, *39*, 2941.
- Nolt, M. B.; Smiley, M. A.; Varga, S. L.; McClain, R. T.; Wolkenberg, S. E.; Lindsley, C. W. *Tetrahedron* **2006**, *62*, 4698.
- The HRV16 3C<sup>pro</sup> coding region was amplified by PCR, subcloned into the pTYB12 expression vector, and transformed into *E. coli* strain BL21(DE3). HRV16 3C<sup>pro</sup> was purified using the IMPACT-CN system (New England Biolabs, Beverly, MA). A protease stock solution was maintained in 20 mM HEPES/NaOH, 100 mM NaCl, 1 mM EDTA, and 1 mM dithiothreitol (pH 7.9).
- Assays were performed at 30 °C in 96-well microplates in reaction volumes of 100  $\mu\text{L}$  with 50 mM Tris (pH 7.6), 1 mM EDTA, 50  $\mu\text{M}$  substrate, 200 nM HRV16 3C<sup>pro</sup>, and various concentrations of test compounds. Inhibitors and enzymes were incubated for 10 min in reaction buffer and reactions were initiated by addition of FRET-substrate. Fluorescence values were monitored at 340 nm (excitation) and 440 nm (emission). Heteroaromatic esters were initially tested at  $1 \mu\text{M}$ . Mean % inhibition was calculated from 3 to 4 repeated experiments.  $IC_{50}$  values of six potent inhibitors were determined using various concentrations with three independent experiments.